Structure and Magnetism of Dibridged Vanadium(IV) Hydrotris(pyrazolyl)borate Dimers

Norman S. Dean,[†] Marcus R. Bond,[‡,†] C. J. O'Connor,[§] and Carl J. Carrano*[,†]

Department of Chemistry, Southwest Texas State University, San Marcos, Texas 78666, and Department of Chemistry, University of New Orleans, New Orleans, Louisiana 70148

Received June 27, 1996[⊗]

The synthesis and characterization of four dinuclear V(IV) complexes are described: **1**, [LVO(μ-$(Ph)_2PO_2$)LVO]; **2**, [LVO(μ-(Ph)HPO_2)$_2$LVO]; **3**, [LVO(μ-OH)$_2$LVO]; and **4**, [LVO(μ-OH)(μ-OAc)LVO] (where L = hydrotris(pyrazolyl)borate). X-ray crystal structural analysis of **1**−**4** gave the following parameters: **1**, $C_{46}H_{46}B_2N_{14}O_6P_2V_2$, $P\bar{1}$, a = 12.249(2) Å, b = 13.951(3) Å, c = 16.391(3) Å, α = 93.95(3)°, β = 100.53(3)°, γ = 110.01(3)°, Z = 2; **2**, $C_{47}H_{48}B_2N_{19}O_9P_3V_3$, $P\bar{1}$, a = 9.927(2) Å, b = 12.307(2) Å, c = 24.878(3) Å, α = 98.12(1)°, β = 100.79(1)°, γ = 91.05(1)°, Z = 2; **3**, $C_{22}H_{28}B_2N_{14}O_4V_2$, *Pbca*, a = 10.698(1) Å, b = 15.414(3) Å, c = 17.865(3) Å, Z = 4; **4**, $C_{24}H_{24}B_2N_{12}O_5V_2$, *C*2/*c*, a = 34.252(4) Å, b = 14.623(2) Å, c = 15.387(2) Å, β = 102.32(1)°, Z = 8. Magnetic measurements indicate that all the compounds except **4** are moderately antiferromagnetically coupled. A rationalization for the magnetic behavior of these and other complexes of this type based on a direct overlap model modulated by the conformation of the eight-membered V(μ-OXO)$_2$V ring is proposed.

Introduction

Over the last several years there has been much interest in magnetic exchange interactions in bridged di-, tri-, and polynuclear metal complexes.[1,2] Much of this interest has been fueled by the desire to design and produce molecular scale magnetic devices.[3−5] Dimeric copper(II) complexes in particular have been extensively studied, and correlations between structure, energies, and type of magnetic exchange were experimentally tested and theoretically explained with suitable models.[6] Although copper(II) and vanadium(IV) systems resemble one another in having only a single unpaired electron in their magnetic orbitals, corresponding magnetostructural relationships have not yet been well developed for the latter metal perhaps due to a dearth of structurally well characterized complexes of the appropriate type. This is particularly unfortunate since a number of these materials, for example, the phosphate-bridged vanadium(IV) solid state species, are of general interest due to the host−guest interactions and catalytic and ion exchange properties exhibited by these materials.[7−9]

Much of the work reported on exchange coupling in vanadium(IV) dimers has concerned the classical vanadyl tartrates.[10−12] A number of other systems have also been examined, but there remains controversy concerning which of the potential interaction pathways dominate.[13−15] Three pathways need to be considered: simple dipolar interaction, direct through space d_{xy}−d_{xy} overlap, and superexchange through bridging ligands. The first is a very small effect and can generally be ignored for bulk magnetic studies while it is difficult to distinguish between the latter two. Indeed both have been invoked at one time or another. In this report we extend our earlier studies[15] on dibridged V(IV) dimers and attempt to provide some rudimentary magnetostructural correlations for this class of compound.

Experimental Section

All synthetic procedures were carried out under an atmosphere of pure dry argon or nitrogen by utilizing standard Schlenk techniques. Subsequent workup was carried out in air unless otherwise noted. Solvents were distilled under nitrogen from the appropriate drying agents (CaH_2 or Na/benzophenone). DMF was Burdick and Jackson "distilled in glass" grade; all other materials were reagent grade and used as received. Potassium hydrotris(pyrazolyl)borate was synthesized according to the reported method,[16] as were [HB(pz)$_3$]VCl_2·DMF, [HB(pz)$_3$]VO(acac),[17] [HB(pz)$_3$]V(μ-O)(μ-OAc)$_2$V HB(pz)$_3$],[18] and [HB(3,5 CH_3pz)$_3$VO(μ-$(C_6H_5O)_2PO_2$)]$_2$.[15]

[HB(pz)$_3$VO(μ-$(C_6H_5)_2PO_2$)]$_2$ (1). [HB(pz)$_3$]VO(acac) (0.76 g, 2.0 mmol) was dissolved in 40−50 mL of CH_3CN. Diphenylphosphonic acid (0.44 g, 2.0 mmol) was then added along with 1−2 mL of H_2O, and the solution was heated. The color gradually changed from pale violet to blue, and a blue solid precipitated. Crystals of **1**, suitable for X-ray analysis, were obtained upon letting the filtrate stand undisturbed for several days at room temperature. The reaction can also be run in dichloromethane as a solvent rather than acetonitrile. In either case the product was isolated by filtration and air-dried. Yield: 0.698 g, 70%. Anal. Calcd for **1**·CH_2Cl_2: C, 47.85; H, 3.92; N, 15.57.

* Corresponding author.
† Southwest Texas State University.
‡ Present address: Department of Chemistry, Southeast Missouri State University, Cape Girardeau, MO 63701.
§ University of New Orleans.
⊗ Abstract published in *Advance ACS Abstracts*, December 1, 1996.

(1) Kahn, O. *Molecular Magnetism*; VCH Publishers: Weinheim, Germany, 1993.
(2) Bertrand, J. A.; Ginsberg, A. P.; Kaplan, R. I.; Kirkwood, C. E.; Martin, R. L.; Sherwood, R. C. *Inorg. Chem.* **1971**, *10*, 240.
(3) Kahn, O. *Nature* **1995**, *378*, 667.
(4) Ferlay, S.; Mallah, T.; Ouahes, R.; Veillet, P.; Verdaguer, M. *Nature* **1995**, *378*, 701.
(5) Kahn, O.; Pei, Y.; Verdaguer, M.; Renard, J. P.; Sletten, J. *J. Am. Chem. Soc.* **1988**, *110*, 782.
(6) Crawford, W. H.; Richardson, H. W.; Wasson, J. R.; Hodgson, D. J.; Hatfield, W. E. *Inorg. Chem.* **1976**, *15*, 2107.
(7) Johnson, D. C.; Jacobson, A. J.; Butler, W. M.; Rosenthal, S. E.; Brody, J. F.; Lewandowski, J. T. *J. Am. Chem. Soc.* **1989**, *111*, 381.
(8) Centi, G.; Trifiro, F.; Edner, J. R.; Francetti, V. M. *Chem. Rev.* **1988**, *88*, 55.
(9) Khan, M. I.; Zubieta, J. *Progress in Inorganic Chemistry*; John Wiley and Sons, Inc.: New York, 1995; pp 1−150.
(10) Garcia-Jaca, J.; Insausti, M.; Cortes, R.; Rojo, T.; Pizarro, J. L.; Arriortua, M. I. *Polyhedron* **1994**, *13*, 357.
(11) Wrobleski, J. T.; Thompson, M. R. *Inorg. Chim. Acta* **1988**, *150*, 269.
(12) Carlisle, G. D.; Simpson, G. D. *J. Mol. Struct.* **1975**, *25*, 219.
(13) Ozarowski, A.; Reinen, D. *Inorg. Chem.* **1986**, *25*, 1704.
(14) Villeneuve, G.; Suh, K. S.; Amoros, P.; Casan-Pastor, N.; Beltran-Porter, D. *Chem. Mater.* **1992**, *4*, 108.
(15) Bond, M. R.; Mokry, L. M.; Otieno, T.; Thompson, J.; Carrano, C. J. *Inorg. Chem.* **1995**, *34*, 11894.
(16) Trofimenko, S. *J. Am. Chem. Soc.* **1967**, *89*, 3170.
(17) Mohan, M.; Holmes, S. M.; Butcher, R. J.; Jasinski, J. P.; Carrano, C. J. *Inorg. Chem.* **1992**, *31*, 2029.
(18) Bond, M. R.; Czernuszewicz, R. S.; Dave, B. C.; Yan, Q.; Mohan, M.; Verastegue, R.; Carrano, C. J. *Inorg. Chem.* **1995**, *34*, 5857.

S0020-1669(96)00770-7 CCC: $12.00

Found: C, 48.14; H, 3.85; N, 15.64. IR (cm^{-1}): 2487(m), 1503, 1404, 1309, 1203, 1138, 1050, 962, 727, 551.

$[HB(pz)_3VO(\mu\text{-}(C_6H_5)HPO_2)]_2$ (2). Synthesis of **2** proceeds as described for **1** except substituting monophenylphosphinic for the diphenylphosphonic acid. Yield: 0.44 g, 52%. Anal. Calcd for **2**: C, 42.79; H, 3.83; N, 19.96. Found: C, 42.47; H, 3.92; N, 20.00. IR (cm^{-1}): 2477(m), 2343(m), 1502, 1405, 1309, 1215, 1186, 1137, 1115, 1053, 966, 764, 716, 620, 568. EPR and electrochemical data for **2** are available in Supporting Information.

$[HB(pz)_3VO(\mu\text{-}OH)]_2$ (3). $[HB(pz)_3]VCl_2$·DMF (1.18 g, 2.0 mmol) was dissolved in acetonitrile and allowed to react with excess 1,8 diazabicyclo[5.4.0]undec-7-ene (1.5 mL). The color gradually darkened and violet crystals of **3** formed overnight. An alternative synthetic route involves the reaction of $[HB(pz)_3]VOCl$·DMF (0.388 g, 1.0 mmol) with NaOH (0.040 g, 1.0 mmol) in 90/10 MeCN/H_2O. Yield: 0.203 g 34%. Anal. Calcd for **3**·4MeCN: C, 41.25; H, 4.53; N, 29.6. Found: C, 40.8; H, 4.21; N, 30.16. IR (cm^{-1}): 3119(m), 2484(m), 1501, 1407, 1308, 1214, 1120, 1049, 967, 761, 720, 620, 549.

$[HB(pz)_3VO(\mu\text{-}OH)(\mu\text{-}OAc)VOHB(pz)_3]$ (4). $[HB(pz)_3]V(\mu\text{-}O)(\mu\text{-}OAc)_2VHB(pz)_3]$ (0.66 g, 1.0 mmol) was dissolved in 75 mL of toluene. The solution was stirred in air for 3 days, during which time the color changed from intense green to a pale violet. A purple crystalline material was obtained by adding 75 mL of hexane and allowing the solution to stand at 0 °C overnight. Crystals of **4**, suitable for X-ray diffraction, were obtained by allowing the initial toluene reaction mixture to stand undisturbed at room temperature for 3 days. Yield: 0.315 g, 50%. Anal. Calcd for **4**·1.25C_7H_8: C, 45.96; H, 4.53; N, 22.38. Found: C, 45.44; H, 4.46; N, 22.08. IR (cm^{-1}): 3119(m), 2484(m), 1542, 1501, 1408, 1308, 1214, 1114, 1055, 967, 761, 720, 620, 550.

Physical Measurements. Routine infrared spectra were obtained on a Perkin-Elmer 1600 FT-IR as KBr pellets. UV−vis spectra were recorded on an HP 8520 diode array spectrophotometer. EPR measurements were made on a Micro-Now 8320 X-band spectrometer. Electrochemical and magnetic susceptibility measurements were made as previously described.[19,20]

Crystallography. Crystals of **1**, **2**, **3**, and **4** were sealed in Lindeman glass capillaries and mounted on a Siemens P4 diffractometer. Unit cell constants were determined by least-squares refinement of the angular settings of 12−30 well-centered high-angle reflections. Structure solution and refinement were achieved using the SHELXTL-PLUS crystallography software from Siemens.[21] Pertinent parameters regarding crystal data, data collection, and structure solution and refinement are summarized in Table 1. Details of individual structural refinements are given below.

$[LVO(\mu\text{-}(C_6H_5)_2PO_2)]_2$ (1). Due to the presence of a weakly bound acetonitrile solvent in the lattice, data crystals of **1** continually deteriorated during data collection despite mounting the crystals in the presence of solvent. Thus, it became necessary to combine several partial data sets (3) and scale them to each other in order to acquire a complete set, which accounts for the relatively poor agreement factors observed.

Nevertheless, a structure solution was achieved via direct methods, and subsequent structure refinement proceeded normally. Anisotropic thermal parameters were refined for all non-hydrogen atoms. Positions of the hydrogen atoms were calculated to give an idealized geometry and fixed to ride on their respective bound atoms except for the position of the hydrogen bound to boron, which was in each case located on the difference map and fixed through the remaining cycles of refinement. A fixed isotropic thermal parameter (0.08 $Å^2$) was assigned to each hydrogen. Selected bond lengths and angles are given in Tables 2 and 3, respectively.

$[LVO(\mu\text{-}(C_6H_5)HPO_2)]_2$ (2). Structure solution and refinement for **2** proceeded normally. The structure contains an acetonitrile of solvation and two independent molecules of the dimer per unit cell. Hydrogen atoms were treated as described above for **1**. Although the phosphorus atoms of the monophenylphosphinate groups in both molecules were disordered, the disorder was easily modeled by two positions with refined occupancy factors. Selected bond lengths and angles are again provided in Tables 2 and 3.

$[HB(pz)_3VO(OH)]_2$ (3). Compound **3** also contained an acetonitrile of crystallization; however, in this case the solvent is held in the lattice by a strong hydrogen bond with one of the bridging hydroxo groups. In addition we were able to obtain the data at low temperature, which resulted in a better overall structure. Hence, structure solution and refinement proceeded normally and anisotropic thermal parameters were refined for all non-hydrogen atoms. Hydrogen atoms were treated as described for **1** with fixed isotropic thermal parameters except that the hydrogen on the bridging hydroxide was located on the difference map and fixed to ride on the oxygen through the remaining cycles of least squares. Pertinent bond lengths and angles are given in Tables 4 and 5, respectively.

{$[HB(pz)_3]_2VO(OH)(OAc)$} (4). Structure solution was again achieved by direct methods, and all of the non-hydrogen atoms of the core structure appeared on the *E*-map. The major remaining peaks found on the difference map were interpreted as an ill-defined toluene of crystallization. This toluene was refined as a rigid body with the C−CH_3 bond length fixed at 1.51 Å and the internal ring C−C bonds at 1.395 Å; however, this refinement resulted in very large thermal parameters, suggesting only partial occupancy. Due to the high correlation between the parameters, a refinement allowing both thermal parameters and site occupancy factors to "float" was also unsuccessful. In the end we first fixed the thermal parameters at a reasonable value and refined the occupancy factor (0.57). The occupancy factor was then fixed and group thermal parameters for the toluene allowed to refine. Hydrogen atoms were not included on the toluene but were placed in idealized positions and fixed to ride on all other appropriate bound atoms with set thermal parameters. Relevant bond lengths and angles can be found in Tables 4 and 5.

Table 1. Crystallographic Data and Data Collection Parameters for **1**−**4**

parameter	**1**	**2**	**3**	**4**
formula	$C_{46}H_{46}B_2N_{14}O_6P_2V_2$	$C_{47}H_{48}B_3N_{19}O_9P_3V_3$	$C_{22}H_{28}B_2N_{14}O_4V_2$	$C_{24}H_{24}B_2N_{12}O_5V_2$
space group	$P\bar{1}$	$P\bar{1}$	*Pbca*	*C*2/c
temp, K	298	298	168	298
a, Å	12.249(2)	9.927(2)	10.698(1)	34.252(4)
b, Å	13.951(3)	12.307(2)	15.414(3)	14.623(2)
c, Å	16.391(3)	24.878(3)	17.865(3)	15.387(2)
α, deg	93.95(3)	98.12(1)		
β, deg	100.53(3)	100.79(1)		102.32(1)
γ, deg	110.01(3)	91.05(1)		
V, $Å^3$	2561.3(8)	2952.8(8)	2946.0(7)	7531.2(11)
ρ_{calc}, g cm^{-3}	1.396	1.463	1.524	1.207
Z	2	2	4	8
fw	1076.4	1301.2	676.1	684.1
μ, cm^{-1}	4.89	6.15	6.91	5.42
R,[a] %	8.32	6.09	6.2	6.28
R_w,[a] %	8.48	6.16	8.23	8.45

[a] Quantity minimized $\omega w(F_o - F_c)^2$, $R = \sum|F_o - F_c|/\omega F_o$. $R_w = (\omega w(F_o - F_c)^2/\sum(wF_o)^2)^{1/2}$.

Table 2. Selected Bond Lengths for **1**, **2(a)**, and **2(b)**

	1	**2(a)**	**2(b)**
V---V	5.27(2)	5.136	5.273
$V-O_{oxo}$	1.582(7)	1.579(10)	1.598(9)
V−O	1.985(4)	1.995(8)	1.990(7)
$V-N_{cis}$	2.113(2)	2.113(9)	2.110(8)
$V-N_{trans}$	2.299(4)	2.318(8)	2.302(11)

Results

Descriptions of Structures. Both compounds **1** and **2** adopt the same basic $[LVO(\mu\text{-}R_2PO_2)]_2$ dinuclear structure seen with the bis(diphenylphosphate)-bridged complexes which we have previously reported (Figures 1 and 2). The vanadium atoms in both structures have distorted octahedral coordination geometry

(19) Bonadies, J. A.; Carrano, C. J. *J. Am. Chem. Soc.* **1986**, *108*, 4088.
(20) O'Connor, C. J. *Prog. Inorg. Chem.* **1982**, *29*, 203.
(21) Sheldrick, G. M. *SHELXTL-PC*, Version 4.1; Siemens X-Ray Analytical Instruments, Inc.: Madison, WI, 1989. Scattering factors from the following: *International Tables for X-Ray Crystallography*; Ibers, J., Hamilton, W., Eds.; Kynoch: Birmingham, U.K., 1974; Vol. IV.

Table 3. Bond Angles (deg) for **1**, **2(a)**, and **2(b)**

1							
O(1)−V(1)−O(2)	100.7(4)	O(1)−V(1)−O(3)	97.6(5)	O(4)−V(2)−O(6)	101.1(4)	O(5)−V(2)−O(6)	100.9(4)
O(2)−V(1)−O(3)	92.1(3)	O(1)−V(1)−N(1)	174.7(4)	O(4)−V(2)−N(8)	84.1(3)	O(5)−V(2)−N(8)	85.8(4)
O(2)−V(1)−N(1)	84.4(4)	O(3)−V(1)−N(1)	83.7(4)	O(6)−V(2)−N(8)	171.4(5)	O(4)−V(2)−N(9)	164.1(3)
O(1)−V(1)−N(3)	98.4(5)	O(2)−V(1)−N(3)	88.3(4)	O(5)−V(2)−N(9)	91.0(4)	O(6)−V(2)−N(9)	94.2(4)
O(3)−V(1)−N(3)	163.7(5)	N(1)−V(1)−N(3)	80.2(5)	N(8)−V(2)−N(9)	80.2(3)	O(4)−V(2)−N(11)	89.4(4)
O(1)−V(1)−N(5)	94.1(5)	O(2)−V(1)−N(5)	164.3(6)	O(5)−V(2)−N(11)	163.8(3)	O(6)−V(2)−N(11)	95.0(5)
O(3)−V(1)−N(5)	91.2(4)	N(1)−V(1)−N(5)	80.7(5)	N(8)−V(2)−N(11)	78.0(4)	N(9)−V(2)−N(11)	84.8(5)
N(3)−V(1)−N(5)	84.3(5)	O(4)−V(2)−O(5)	90.4(4)				
2(a)							
O(7)−V(2)−O(6)	90.2(3)	O(7)−V(2)−N(11)	164.3(3)	O(5)−V(1)−N(1)	89.4(3)	N(5)−V(1)−N(1)	79.7(4)
O(6)−V(2)−N(11)	94.5(3)	O(7)−V(2)−O(2)	101.1(4)	O(5)−V(1)−O(4)	88.4(3)	N(5)−V(1)−O(4)	82.1(3)
O(6)−V(2)−O(2)	99.8(3)	N(11)−V(2)−O(2)	92.9(4)	N(1)−V(1)−O(4)	161.7(4)	O(5)−V(1)−O(1)	101.3(4)
O(7)−V(2)−N(9)	85.5(3)	O(6)−V(2)−N(9)	163.2(3)	N(5)−V(1)−O(1)	172.8(4)	N(1)−V(1)−O(1)	97.3(4)
N(11)−V(2)−N(9)	85.7(3)	O(2)−V(2)−N(9)	97.0(4)	O(4)−V(1)−O(1)	100.9(4)	O(5)−V(1)−N(3)	164.4(3)
O(7)−V(2)−N(7)	86.5(3)	O(6)−V(2)−N(7)	82.1(3)	N(5)−V(1)−N(3)	79.2(4)	N(1)−V(1)−N(3)	87.1(4)
N(11)−V(2)−N(7)	79.3(3)	O(2)−V(2)−N(7)	172.1(4)	O(4)−V(1)−N(3)	90.1(4)	O(1)−V(1)−N(3)	94.2(4)
N(9)−V(2)−N(7)	81.4(3)	O(5)−V(1)−N(5)	85.3(3)				
2(b)							
N(17)−V(3)−O(3)	93.9(4)	N(17)−V(3)−N(15)	85.8(3)	N(15)−V(3)−O(9)	89.9(3)	O(8)−V(3)−O(9)	91.7(3)
O(3)−V(3)−N(15)	95.1(4)	N(17)−V(3)−O(8)	88.5(3)	N(17)−V(3)−N(13)	80.7(4)	O(3)−V(3)−N(13)	172.2(4)
O(3)−V(3)−O(8)	101.5(4)	N(15)−V(3)−O(8)	162.7(4)	N(15)−V(3)−N(13)	79.0(4)	O(8)−V(3)−N(13)	84.0(4)
N(17)−V(3)−O(9)	165.7(4)	O(3)−V(3)−O(9)	100.1(4)	O(9)−V(3)−N(13)	85.1(3)		

Table 4. Selected Bond Lengths (Å) for **3** and **4**

3			
V(1)−O(1)	1.602 (4)	V(1)−N(1)	2.101 (5)
V(1)−O(2)	2.016 (6)	V(1)−N(3)	2.127 (5)
V(1)−O(2)	2.004 (4)	V(1)−N(5)	2.388 (5)
V(1)−O(2A)	1.979 (4)	V(1)−V(1A)	3.122 (5)
4			
V(1)−O(4)	1.599 (5)	V(1)−N(8)	2.119 (6)
V(2)−O(3)	1.574 (6)	V(2)−N(4)	2.129 (7)
V(1)−O(5)	1.995 (4)	V(2)−N(5)	2.118 (7)
V(2)−O(1)	2.008 (5)	V(2)−N(6)	2.321 (6)
V(2)−O(5)	1.974 (5)	V(1)−N(10)	2.294 (6)
V(1)−N(7)	2.094 (6)	V(1)−V(2)	3.620 (7)

Table 5. Selected Bond Angles (deg) for **3** and **4**

3			
O(1)−V(1)−O(2)	101.7(2)	N(1)−V(1)−N(5)	78.7(2)
O(1)−V(1)−N(1)	94.9(2)	N(3)−V(1)−N(5)	75.9(2)
O(2)−V(1)−N(1)	91.8(2)	O(1)−V(1)−O(2A)	101.7(2)
O(1)−V(1)−N(3)	91.3(2)	O(2)−V(1)−O(2A)	76.8(2)
O(2)−V(1)−N(3)	166.8(2)	N(1)−V(1)−O(2A)	161.4(2)
N(1)−V(1)−N(3)	89.3(2)	N(3)−V(1)−O(2A)	98.6(2)
O(1)−V(1)−N(5)	165.7(2)	N(5)−V(1)−O(2A)	86.9(2)
O(2)−V(1)−N(5)	91.3(2)	V(1)−O(2)−V(1A)	103.2(2)
4			
O(2)−V(1)−O(4)	98.5(2)	O(1)−V(2)−O(5)	91.1(2)
O(2)−V(1)−O(5)	90.5(2)	O(3)−V(2)−O(5)	100.9(3)
O(4)−V(1)−O(5)	102.2(2)	O(1)−V(2)−N(4)	86.6(3)
O(2)−V(1)−N(7)	164.8(2)	O(3)−V(2)−N(4)	95.5(3)
O(4)−V(1)−N(7)	96.0(3)	O(5)−V(2)−N(4)	163.6(2)
O(5)−V(1)−N(7)	90.7(2)	O(1)−V(2)−N(5)	164.2(3)
O(2)−V(1)−N(8)	88.5(2)	O(3)−V(2)−N(5)	95.1(3)
O(4)−V(1)−N(8)	93.2(2)	O(5)−V(2)−N(5)	93.6(2)
O(5)−V(1)−N(8)	164.5(2)	N(4)−V(2)−N(5)	84.5(3)
N(7)−V(1)−N(8)	86.3(2)	O(1)−V(2)−N(6)	86.4(2)
O(2)−V(1)−N(10)	84.1(2)	O(3)−V(2)−N(6)	172.9(3)
O(4)−V(1)−N(10)	171.4(2)	O(5)−V(2)−N(6)	83.7(2)
O(5)−V(1)−N(10)	85.9(2)	N(4)−V(2)−N(6)	79.9(3)
N(7)−V(1)−N(10)	80.9(2)	N(5)−V(2)−N(6)	79.2(2)
N(8)−V(1)−N(10)	78.6(2)	V(1)−O(5)−V(2)	131.6(3)
O(1)−V(2)−O(3)	98.8(3)		

with three of the four available terminal sites occupied by a tris(pyrazolyl)borate group. The remaining terminal ligand is the ubiquitous oxo group which in all cases adopts an anti configuration in the dimer. The remaining two sites on each vanadium are filled by oxygen atoms of the bridging diphenylphosphonate or monophenylphosphinate groups. Both structures contain two independent molecules in the unit cell. For **1** both molecules have inversion site symmetry so that only one half of each dimer is unique; however, their overall structures are very similar, hence only mean values for bond lengths are compiled in Table 2. In **2**, on the other hand, one of the molecules has inversion site symmetry with only one half of the dimer unique while the second molecule is a complete dimer with no crystallographically imposed symmetry. In addition, since the monophenylphosphinate is an unsymmetrical bridging ligand, two possible isomeric structures are possible, one with the phenyl groups syn to each other in the dimer and one with them anti. Only the anti geometry is found in both molecules of **2**, the difference between them being only in the conformation of the $V(OPO)_2V$ ring (*vide infra*).

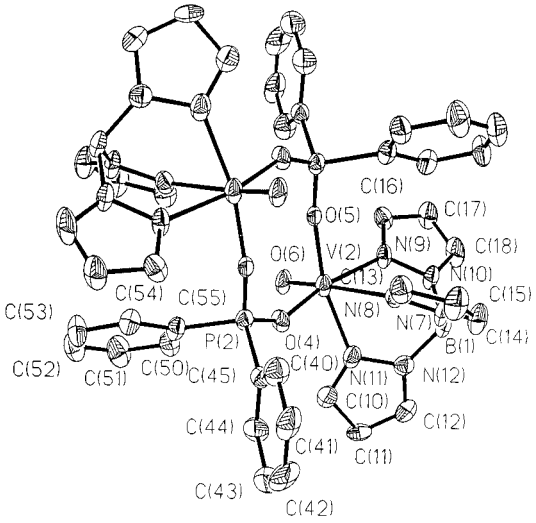

Figure 1. ORTEP diagram (30% probability ellipsoids) with atom labeling scheme for one of the two independent molecules of **1**.

Despite the similarities within this family of structures there are also some notable differences. Most obvious of these is the range of V---V distances observed in the four dimers structurally characterized so far. The diphenylphosphonate dimer has V---V distances which are very similar between the two independent molecules and average 5.27(2) Å. The geometries of the two independent molecules in the monophenylphosphinate structure differ considerably, with one having a V---V distance of 5.27 Å, a value similar to that seen in **1**, while

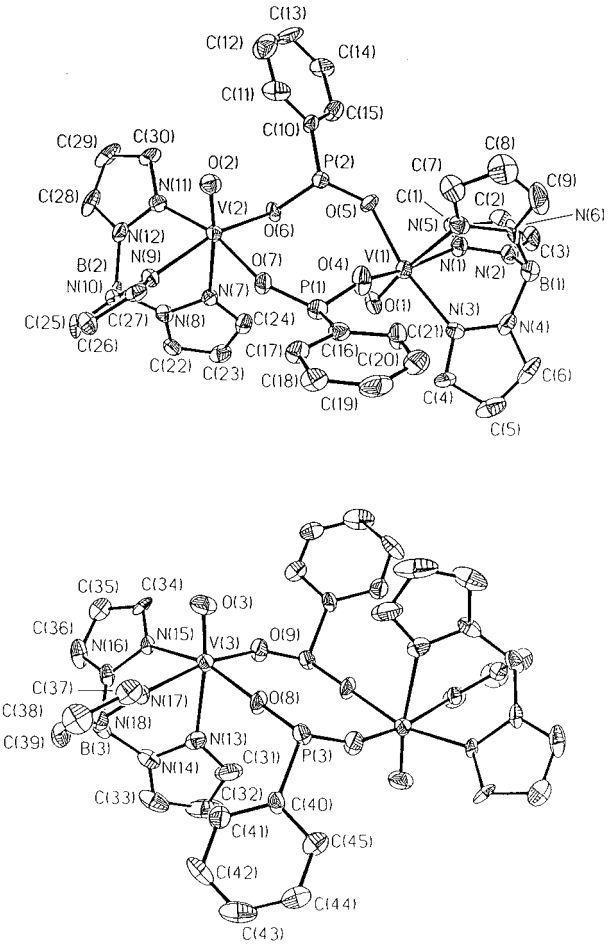

Figure 2. ORTEP plot (30% probability spheres) with atom labeling scheme for both molecules of **2**.

the other has the vanadiums more than 0.1 Å closer at 5.14 Å. Since neither the P−O nor V−O bonds are significantly different in the four structures, the differences in the V---V distances can be attributed to differing geometries of the eight-membered $V(OPO)_2V$ rings. The geometry of the ring varies from the nearly chair configuration seen with the diphenylphosphate-bridged complex previously reported, where the dihedral angle between the VO_2 and PO_2 planes is 128.4° (120° ideal), to nearly planar in one of the molecules of **2** where the angle is 171.9° (180° ideal). The (3,5-dimethylpyrazolyl)borate analog of the diphenylphosphate-bridged dimer and both molecules of **1** have intermediate values of the dihedral angle (164.7° and 167°, respectively) but lie closer to the planar than the chair conformation. For reasons that are not entirely clear, the eight-membered ring in the second molecule of **2** is quite distorted but is closer to the chair conformation.

Figure 3 shows the structure of $\{HB(C_3N_2H_3)_3\}_2V_2O_2(OH)_2$, which contains two vanadium(IV) centers in a distorted octahedral environment composed of a facially coordinating tris(pyrazolylborate) ligand, a terminal oxo group, and two bridging hydroxide ligands. Also notable are the acetonitriles of crystallization, which are strongly hydrogen bonded to the bridging hydroxides (N···H, 2.065 Å; N···H−O angle, 173.2°). This interaction has the effect of pulling the hydroxide hydrogen out of the V−O−V plane and pyramidalizing the oxygen (sum of the angles around O2 = 337° rather than 360°). The complex itself has a crystallographically imposed inversion center resulting in an anti configuration for the two vanadyl oxygen atoms. The V═O bond length is 1.602(4) Å, while the V−OH bond distances are significantly longer at 2.004(4) Å. Two distinct vanadium−nitrogen bond distances are present in the

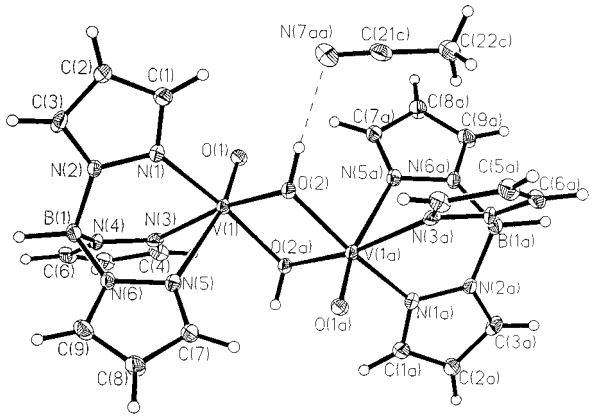

Figure 3. ORTEP diagram (30% probability ellipsoids) with atom labeling scheme for **3**.

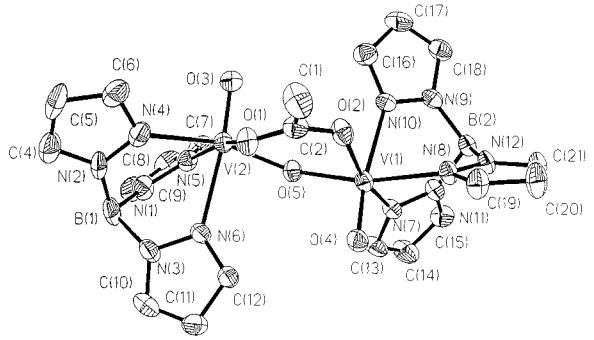

Figure 4. ORTEP diagram (30% probability ellipsoids) with atom labeling scheme for **4**.

complex with those trans to the bridging hydroxide found at an average distance of 2.114 Å, while the nitrogen trans to the terminal oxo ligand is significantly longer at 2.388(5) Å. The angles within the V_2O_2 bridging unit are 103.2(2)° (V−O−V) and 76.8(2)° (O−V−O), with the resulting vanadium−vanadium separation, 3.122 Å. The structural parameters of **3** are similar, but not identical, to those of a closely related system containing the tridentate triazacyclononane ligand instead of the tris(pyrazolylborate).[22] In the TACN complex for instance the V−O(H) distances are 1.96 Å and the resulting metal−metal separation is shorter at 3.033 Å. These differences are likely due to the Coulombic repulsion generated by the negative charge of the tris(pyrazolylborate) ligands, as compared to the neutral TACN, as well as to the strong hydrogen bonding of the acetonitriles of crystallization to the bridging hydroxides in **3**.

The structure of **4** is similar to that of **3**, except that a bidentate acetate bridge substitutes for one of the hydroxo bridges in the latter (Figure 4). The molecule no longer possesses inversion symmetry but contains instead a noncrystallographic C_2 axis passing through the two acetate carbons and the hydroxo oxygen. In order to accommodate the increased bite of the acetate ligand the V−OH−V angle has opened up from 103 to 131° with a resulting increase in the V---V distance from 3.12 to 3.62 Å. In order to minimize the distortion of the V−OH−V unit, the acetate bridge is not coplanar with the hydroxide but rather is twisted by some 22.6°. This in turn results in a twisting of the V═O vectors, which, although still primarily anti, are now twisted with respect to each other by some 27°.

Magnetic Measurements. The magnetic data for **1**−**3** and for $[HB(3,5CH_3pz)_3VO(C_6H_5O)_2PO_2]_2$ over the temperature

(22) Wieghardt, K.; Bossek, U.; Volckmar, K.; Swiridoff, W.; Weiss, J. *Inorg. Chem.* **1984**, *23*, 1387.

Table 6. Fitted Parameters to Heisenberg−Van Vleck−Dirac Isotropic Exchange Model

	1	**2**	**3**	unsubstituted[a] phosphate	3,5-dimethyl phosphate
J, K	−11.75(8)	−40.65(1)	−38.8(1)	+2.2(3)	−27.2(3)
g	1.982(1)	1.869(1)	1.768(1)	1.918(5)	2.116(4)
% impurity	1.6(4)	1.1(2)	1.8(2)	na[b]	5.4(1.2)
norm	0.0325	0.01791	0.01745	na	0.09899

[a] From ref 15. [b] Not available.

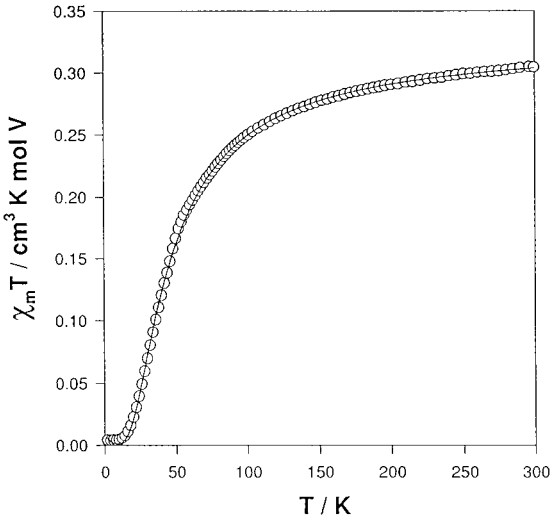

Figure 5. Plot of χT vs T for **1** (open circles) with the fit to the equation described in the text (solid line).

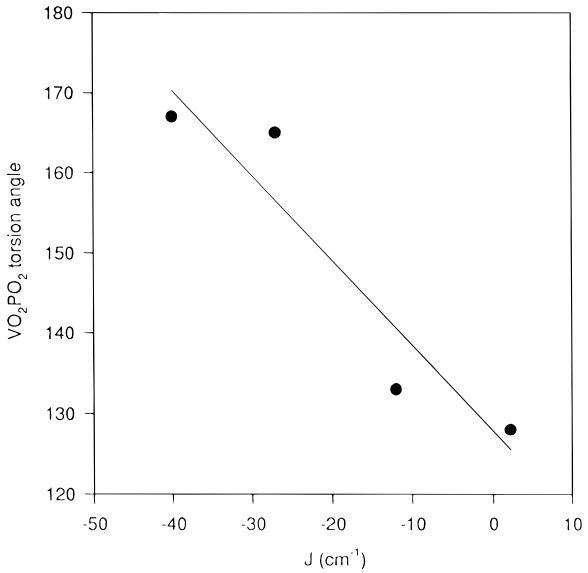

Figure 6. Plot of the dihedral angle between the VO_2 and PO_2 planes of the $V(OPO)_2V$ ring and the magnitude of J.

range 2−300 K are all qualitatively similar with μ_{eff} decreasing gradually from about 1.78 μ_B at room temperature to near 0 at 2 K. Such behavior is consistent with moderate antiferromagnetic coupling between the two d^1 vanadium centers in the dimer. All the data could be satisfactorily fitted to Heisenberg−Van Vleck−Dirac, HVD, isotropic spin exchange Hamiltonian, $H = -2JS_1 \cdot S_2$, with $S_1 = S_2 = {}^1/_2$ and a monomeric paramagnetic impurity correction term. An example of the quality of the fit is given in Figure 5, and the fits are summarized in Table 6. The data for compound **4** did not resemble that of the other compounds in this series; instead, μ_{eff} dropped almost monotonically from a room temperature value which suggested ferromagnetic coupling between the vanadium centers, until it reached a plateau value near 1.79 μ_B/V (the uncoupled limit) at ca. 20 K. As of yet we are unable to satisfactorily account for this behavior although we have reproduced it from several samples, and microscopic evaluation suggests no heterogeneity in them. Further work is in progress.

Discussion

It is probably useful to separate the discussion of magneto-structural effects for the phosphate/phosphonate/phosphinate bridge dimers from that of the hydroxo-bridged species **3** and **4**. As alluded to earlier, there has been considerable interest in establishing a correlation between structural geometry and magnetic exchange in vanadium phosphate solid state materials and some success has been achieved.[23−25] However, these studies are based on solid state materials containing numerous structural elements, making it difficult to pin down which of these elements give rise to bulk magnetic properties. Hence, the simple dimers prepared in this and our previous study are particularly valuable. We have attempted to correlate the degree of magnetic coupling with various structural parameters, and the best correlation found is with the conformation of the eight-membered $V(OPO)_2V$ ring. As measured by the dihedral angle between VO_2 and PO_2 planes, an ideal chair conformation would have a dihedral angle of 120° while the planar conformation is characterized by an angle of 180°. The quasi-linear correlation between this angle and the magnitude of J is shown in Figure 6.

The canting of the two vanadyl basal planes with respect to each other has been proposed to correlate with the sign and magnitude of the magnetic coupling constant in certain intercalated solid state V(IV) phosphates.[25] However, there is no such correlation here as, for example, **1** and both the 3,5-dimethyl-substituted and unsubstituted tris(pyrazolyl)borate phosphate-bridged dimers all have their vanadyl basal planes exactly parallel by symmetry, and yet the three vary widely in J. Such a correlation can be explained, rather, using the direct overlap model we proposed in our previous work.[15] In this model a ferromagnetic interaction is expected in the chair conformation through direct overlap of the d_{xy} magnetic orbital on one metal with the V═O π-system of the other (the V═O π-orbital is orthogonal to the d_{xy} magnetic orbital). As the chair geometry is bent back toward the planar archetype, the d_{xy}-V═O π-overlap will diminish while the $d_{xy}-d_{xy}$ overlap will increase to yield an overall antiferromagnetic interaction.

If the direct overlap pathway is operative, then there is also expected to be a distance dependence to the magnitude of the magnetic coupling. A comparison of the J values for **1** and the 3,5-dimethyl phosphate-bridged derivative would seem to support this view. Both complexes adopt a near planar configuration of the $V(OPO)_2V$ ring, but the AFC is much larger for **1** due to the shorter V---V distance. One other complex with a $V(OXO)_2V$ core geometry is known. In this case the

(23) Beltran-Porter, D.; Amoros, P.; Ibanez, R.; Martinez, E.; Beltran-Porter, A. *Solid State Ionics* **1989**, *32*, 57.
(24) Beltran-Porter, D.; Beltran-Porter, A.; Amoros, P.; Ibanez, R.; Martinez, E. *Eur. J. Solid State Chem.* **1991**, *28*, 131.
(25) Papoutsakis, D.; Jackson, J. E.; Nocera, D. G. *Inorg. Chem.* **1996**, *35*, 800.

bridging ligand is acetate and the eight-membered ring adopts a boat rather than chair or planar configuration due to the syn arrangement of the vanadyl units.[26] In this geometry direct orbital overlap between the d_{xy} orbitals is still possible, and hence an AFC can be expected and indeed is observed. The short (4.075 Å) V---V distance in this complex leads directly to a strong coupling, $J = -114$ cm^{-1}.

Unlike the related Cu(II) systems which have $d_{x^2-y^2}$ as the magnetic orbital, the magnetic orbital in most oxo V(IV) species is the d_{xy}. An excellent pathway for superexchange in Cu(II) dimers exists because the $d_{x^2-y^2}$ orbital points directly toward the bridging ligand groups. In contrast the orbital lobes on two adjacent V(IV) ions are aligned and can in principle lead to direct overlap. Indeed the direct overlap mechanism has been involved as the primary path for magnetic coupling in bis(μ-hydroxo, alkoxo, phenolato, and carboxylato) V(IV) complexes.[22,26,27] In addition, acetate and presumably phosphate as well have been reported to mediate only a very weak (a few cm^{-1}) superexchange coupling. However, solid state NMR data has been presented to suggest that superexchange through bridging phosphates may be important and that the degree of shift in the ^{31}P NMR signal correlates with the magnitude of J.[14] A combination of superexchange with the direct overlap model can also explain the observed correlations. In this case, in the retracted chair conformation, the FM coupling by direct exchange through the vanadyl oxygen is larger than any AFM coupling through the phosphates. However, as the ring flattens, the direct exchange progressively becomes more AFM and combines with the AFM superexchange through the bridge to give an overall AFM coupling. Solid state ^{31}P NMR experiments are needed to confirm this model, and such are in progress.

A few μ-hydroxo, alkoxo, phenolato edge-sharing bioctahedral V(IV) complexes which have had both their structures and magnetic properties determined are also known.[26−29] Two new examples, **3** and **4**, are presented here. These complexes have obvious analogies with the Cu(II) hydroxo-bridged dimers where a well-defined magneto structural correlation is available. Here a single-degree change in the bridge angle results in a variation of about 74 cm^{-1} in the singlet−triplet separation.[7] Examination of four such complexes including **3** containing syn or anti-orthogonal vanadyl units unfortunately fails to reveal any such simple correlation with bridging angle or internuclear separation. However, it is clear that the coupling in **3** is anomalously low (i.e., −40 vs ca. −150(20) cm^{-1}) compared to that seen in the related complexes. We attribute this to the hydrogen bonding between the acetonitrile and the bridging hydroxide on **3** which bends the hydroxyl hydrogen out of the V−O−V plane, leading to a more sp^3-like hybridized oxygen. Such an oxygen is expected to have a reduced efficiency for superexchange-mediated coupling. A recent report also shows that, by changing the geometry of the vanadyl units to syn or anti coplanar or twist, a reversal of sign from AFM to FM is possible.[29] Such a twist may be important in explaining the anomalous magnetic behavior of **4**.

Acknowledgment. This work was supported by Grants AI-1157 from the Robert A. Welch Foundation and SF-93-12 from the Dreyfus Foundation. The NSF-ILI program grant USE-9151286 is acknowledged for partial support of the X-ray diffraction facilities at Southwest Texas State University.

Supporting Information Available: Atomic positions, bond lengths and angles, anisotropic displacement parameters, hydrogen atom coordinates, data collection, and crystal structure parameters for **1**−**4** along with EPR spectra and cyclic voltammetric data for **2** (44 pages). Ordering information is given on any current masthead page.

IC9607705

(26) Koppen, M.; Fresen, G.;Wieghardt, K.; Llusar, R. M.; Nuber, B.; Weiss, J. *Inorg. Chem.* **1988**, *27*, 721.
(27) Carrano, C. J.; Nunn, C. M.; Quan, R.; Bonadies, J. A.; Pecoraro, V. L. *Inorg. Chem.* **1990**, *29*, 944.
(28) Neves, A.; Wieghardt, K.; Nuber, B.; Weiss, J. *Inorg. Chim. Acta* **1988**, *150*, 183.
(29) Plass, W. *Angew. Chem., Int. Ed. Engl.* **1996**, *35*, 627.